Single-spin asymmetries and invariant cross sections of the high transverse-momentum inclusive π^0 production in 200 GeV/c pp and $\overline{pp}$ interactions

D. L. Adams,[1] N. Akchurin,[2] N. I. Belikov,[3] A. Bravar,[14,*] J. Bystricky,[4] M. D. Corcoran,[1] J. D. Cossairt,[5] J. Cranshaw,[1] A. A. Derevschikov,[3] H. En'yo,[6] H. Funahashi,[6] Y. Goto,[6] O. A. Grachov,[3] D. P. Grosnick,[7] D. A. Hill,[7] T. Iijima,[6,†] K. Imai,[6] Y. Itow,[6] K. Iwatani,[8] K. W. Krueger,[9] K. Kuroda,[10] F. Lehar,[4] A. de Lesquen,[4] D. Lopiano,[7] F. C. Luehring,[11,‡] T. Maki,[12] S. Makino,[6] A. Masaike,[6] Yu. A. Matulenko,[3] A. P. Meschanin,[3] A. Michalowicz,[10] D. H. Miller,[11] K. Miyake,[6] T. Nagamine,[6,§] F. Nessi-Tedaldi,[1,‖] M. Nessi,[1,‡] C. Nguyen,[1,¶] S. B. Nurushev,[3] Y. Ohashi,[7,**] Y. Onel,[2] D. I. Patalakha,[3] G. Pauletta,[13] A. Penzo,[14] A. L. Read,[5] J. B. Roberts,[1] L. van Rossum,[5] V. L. Rykov,[3] N. Saito,[6] G. Salvato,[15] P. Schiavon,[14] T. Shima,[7] J. Skeens,[1] V. L. Solovyanov,[3] H. Spinka,[7] R. W. Stanek,[7] R. Takashima,[16] F. Takeutchi,[17] N. Tamura,[18] N. Tanaka,[19,††] D. G. Underwood,[7] A. N. Vasiliev,[3] J. L. White,[1,‡‡] S. Yamashita,[6] A. Yokosawa,[7] T. Yoshida,[20] and A. Zanetti[14]

(FNAL E704 Collaboration)

[1]*T. W. Bonner Nuclear Laboratory, Rice University, Houston, Texas 77251*
[2]*Department of Physics, University of Iowa, Iowa City, Iowa 52242*
[3]*Institute for High Energy Physics, 142284, Protvino, Russia*
[4]*CEN-Saclay, F-91191 Gif-sur-Yvette, France*
[5]*Fermi National Accelerator Laboratory, Batavia, Illinois 60510*
[6]*Department of Physics, Kyoto University, Kyoto 606, Japan*
[7]*Argonne National Laboratory, Argonne, Illinois 60439*
[8]*Hiroshima University, Higashi-Hiroshima 724, Japan*
[9]*Northeastern State University, Talequah, Oklahoma 74464*
[10]*Laboratoire de Physique des Particules, B.P.909, F-74017 Annecy-le-Vieux, France*
[11]*Physics Department, Northwestern University, Evanston, Illinois 60201*
[12]*University of Occupational and Environmental Health, Kita-Kyushu 807, Japan*
[13]*University of Udine, I-33100 Udine, Italy*
[14]*Dipartimento di Fisica, Universita di Trieste, I-34100 Trieste, Italy*
[15]*Dipartimento di Fisica, Universita di Messina, I-98100 Messina, Italy*
[16]*Kyoto University of Education, Kyoto 612, Japan*
[17]*Kyoto-Sangyo University, Kyoto 612, Japan*
[18]*Okayama University, Okayama 700, Japan*
[19]*Los Alamos National Laboratory, Los Alamos, New Mexico 87545*
[20]*Osaka City University, Osaka 558, Japan*

(Received 24 March 1995)

The π^0 inclusive and semi-inclusive, single-spin asymmetries have been measured using transversely polarized, 200-GeV/c proton and antiproton beams colliding with an unpolarized hydrogen target. The measured asymmetries are consistent with zero within the experimental uncertainties for the kinematic region $-0.15<x_F<+0.15$ and $1<p_T<4.5$ GeV/c. Improvements in the data analysis showed that our earlier large asymmetries at $p_T>3$ GeV/c were not correct. These data indicate that PQCD expectations seem confirmed and the higher-twist contribution to the single-spin asymmetry in π^0 production at $x_F=0$ is not large. Additional evidence for such a conclusion comes from the measurement of a semi-inclusive π^0 asymmetry, where associated charged particles are detected opposite to the π^0 azimuthal direction. This experiment also provides high-statistics data on the inclusive π^0 cross sections for pp and $\overline{pp}$ collisions at $\sqrt{s}\approx 19.4$ GeV.

PACS number(s): 13.88.+e, 13.85.Ni

*Present address: University of Iowa, Iowa City, IA 52242.
†Present address: National Laboratory for High Energy Physics (KEK), Japan.
‡Present address: Indiana University, Bloomington, IN 47405
§Present address: Bubble Chamber Physics Laboratory, Tohoku University, Sendai 980, Japan.
‖Present address: CERN, CH-1211 Geneva 23, Switzerland.
¶Present address: University of Texas, Austin, TX 78712.
**Present address: Japan Synchrotron Radiation Research Institute, Hyogo, 678-12, Japan.
††Deceased.
‡‡Present address: American University, Washington, D.C. 20016.

I. INTRODUCTION

There has been a recent growing interest in the measurement of single transverse spin asymmetries in inclusive reactions, due to the discovery of a large left-right asymmetry in the inclusive production of pions at 13 and 18 GeV/c, [1] 24 GeV/c, [2] and 40 GeV/c, [3] and the measurement of a large polarization in the production of hyperons [4]. Since in perturbative QCD any single transverse spin effect is proportional to small parameters [5], such as the strong coupling constant α_S, quark mass m_q, and inverse energy $1/\sqrt{s}$, then, at sufficiently high energy, the expected spin effects become less than 1%. However, the data indicate spin effects on the order of 10%. Methods of reconciling such an apparent contradiction were proposed in several theoretical papers, for example, quark-gluon correlations [6] and the color string model [7]. Some theoretical models differ in their predictions for the single transverse spin asymmetry by an order of magnitude; for example, compare Refs. [8] and [9] for direct photon production. The above model-dependent approaches give different predictions, and new experimental data at higher p_T in a wide x_F range are needed for input to these models.

The single transverse spin asymmetries for inclusive and semi-inclusive π^0 production were measured in the E-704 experiment at Fermilab using 200-GeV/c polarized beams of protons or antiprotons and an unpolarized liquid hydrogen target. The transverse momenta of the scattered particles were between 1 and 4.5 GeV/c. The QCD predictions may be applicable at the highest measured p_T values. The reliability of the data that were used to calculate the asymmetry has been checked by several methods described hereafter. All the systematics in the experiment were checked and as a result the cross sections were derived. Preliminary results were published [10] indicating large pp asymmetries for $p_T > 3$ GeV/c. After some improvements in the data analysis described in detail in the text, the present results in this region are now consistent with zero.

The setup of the experiment and the data analysis are described in Sec. II. Section III presents the invariant cross sections for both pp and $\overline{p}p$ interactions, and the single-spin asymmetries are presented in Sec. IV. Section V is devoted to the discussion of the results.

II. EXPERIMENTAL SETUP AND DATA ANALYSIS

The Fermilab polarized proton (antiproton) beam with 200 GeV/c momentum was produced using the parity-violating decays of Λ ($\overline{\Lambda}$) hyperons. The incoming 800-GeV/c primary-proton beam from the Fermilab Tevatron struck a beryllium target and created unpolarized Λ's. The intensity of Λ hyperons was maximized by centering the beam-line acceptance at zero production angle. In the unpolarized Λ rest frame, the decay $\Lambda \rightarrow p + \pi^-$ occurs isotropically and the decay-proton polarization is about 65% with the spin direction along the proton momentum. In the laboratory reference frame, the trajectories of the protons from the Λ decays can be traced back to the plane of the production target. Protons with components of their momentum transverse to the Λ direction appear to come from a virtual source displaced from the actual Λ source. The beam-tagging system was designed and installed at the intermediate focus of the beam channel to tag electronically the polarization for each proton in the 200-GeV/c beam by using a correlation between the position of a proton relative to the beam axis and the proton polarization. The particle tagging measures only the horizontal component of the transverse proton polarization. The beam-transport system had been designed to minimize beam depolarization effects. The 200-GeV/c polarized protons then struck a hydrogen target after their spins were rotated from horizontal to vertical by spin-rotation magnets. The total number of protons that reached the experimental target with a $\pm$ 9% momentum bite was about 3×10^7, when 3×10^{12} primary protons per 20 s spill were incident on the production target. A polarized-antiproton beam was made in a completely analogous manner to the polarized-proton beam. The only change to the beam line when producing polarized antiprotons was to reverse the polarities of both dipole and quadrupole magnets. Further details on the polarized beam line are described in Ref. [11].

The beam-tagging system, composed of several scintillator hodoscopes, determined the momentum and polarization of individual beam particles, and allowed a selection of beam particles within definite intervals of these quantities. A total of 13 bins covered the -65% to $+65\%$ polarization range in 10% intervals. Beam protons (antiprotons) with polarization values between $+35\%$ and $+65\%$ were designated as ''positive,'' those between -35% and -65% as ''negative,'' and those between -35% and $+35\%$ as ''zero.'' The average polarization values for these regions were $+46\%$, -46%, and zero, respectively. The flux of beam particles incident on the target was measured by a similar hodoscope system. The beam-tagging system assigned a polarization value for each beam particle relative to a known trajectory. An absolute measurement of the beam polarization was necessary to confirm those values. Two independent measurements with two different polarimeters agreed with the expected polarization value of 46% [12,13].

A spin rotator, loosely called a ''snake,'' consisted of a set of 12 dipole magnets that changed the beam-particle polarization state from one direction to another. In fact, only eight magnets were used for the single-spin asymmetry measurements. The design had no overall perturbation of the beam-particle trajectory; the bends and displacements of the particle trajectory canceled during passage through the snakes. A spin rotator was used in the beam line for two reasons: (1) to periodically reverse the polarization direction to decrease experimental systematic errors and (2) to change the spin direction from the transverse horizontal direction, in which the beam particle spin component was actually tagged, to the transverse vertical direction for the experimental measurements of interest. The net spin rotation was in the same direction for both protons and antiprotons.

The experimental layout is shown in Fig. 1. Trajectories of each beam particle impinging on a 100-cm liquid hydrogen target were defined by beam hodoscopes and multiwire proportional chambers, located upstream and downstream of the snake magnets. Photons from the decays of neutral mesons produced in the target were detected in two central electromagnetic calorimeters CEMC1 and CEMC2 located symmetrically to the left and to the right of the beam axis at

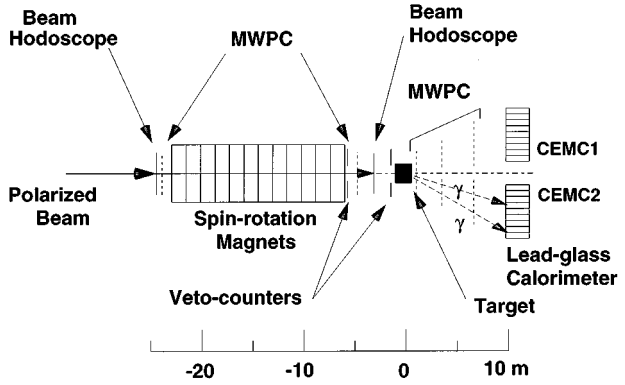

FIG. 1. Layout of the experimental apparatus. Note that the scales on the two axes are different.

10 m from the target. Each calorimeter is an array of 504 lead-glass counters, stacked in 21 columns by 24 rows. The dimensions of each lead-glass block were 3.81 cm $\times$ 3.81 cm $\times$ 45 cm (18 radiation lengths). Each array covered a polar angle of $(5.5\pm 2.2)°$ in the laboratory frame, where the 5.5° angle corresponds to 90° c.m., and azimuthal angles of $\pm$ 25° with respect to the horizontal plane containing the beam axis.

Three sets of proportional wire chambers (MWPC in Fig. 1), located between the target and each CEMC, were used for charged particle detection and track reconstruction. The first set, 1 m downstream from the center of the target, consisted of four planes (two X and two Y) with 256 wires in each plane, and whose area covered both CEMC's. The second set, 3.3 m downstream of the target, consisted of three planes with 256 wires in the first two planes (X and Y) and 320 wires in the third plane (V, tilted at $-28°$). The third set, 6.7 m downstream of the target, consisted of four planes with a total of 2052 wires. Planes U and V were tilted at 28° and $-28°$, respectively. The second and the third multiwire proportional chamber (MWPC) sets were divided to left and right parts for CEMC1 and CEMC2, accordingly. All wire planes had 2 mm spacing. During normal operation of all the chambers, up to 60% of the events had a reconstructed vertex located in the hydrogen target.

The calibration of the CEMC was carried out with an $E_0 = 30$ GeV positron beam. The coefficients c_i, which transform the signal amplitudes A_{il} into energies E_{il} by

$$E_{il} = c_i \cdot A_{il}, \tag{1}$$

where i is a counter number and l is an event number, were defined as a result of this calibration. The c_i were defined by minimizing the quantity

$$\sum_l \left(\sum_i E_{il} - E_0 \right)^2. \tag{2}$$

The details of the solution of these equations are described elsewhere [14]. An energy resolution of 7% [full width at half maximum (FWHM)] at 30 GeV was achieved with this method. This resolution was expected for this type of calorimeter. The lead-glass spatial resolution ± 1.5 mm was determined in special measurements with a 30-GeV positron beam by comparing the value of the center of gravity of an electromagnetic shower with a coordinate in the MWPC located in front of the CEMC.

In addition to the method described above, further analysis has provided an improved calibration method using π^0 and η events. The previous results [10] used only the calibration coefficients obtained from (1) and (2). In the new analysis, photon pairs in the effective mass regions of the π^0 and η were required to have the meson mass value for all p_T. Corrections to the calibration coefficients obtained with the positron beam varied from 1% to 5% for the different data-taking periods.

Signals from all phototubes of lead-glass counters in each calorimeter array went to the front-end electronics. A small part of each signal (5%) went to trigger electronics consisting of two levels. First, all the trigger signals were summed and then amplified for each CEMC column separately. Second, the resulting signals for the 21 columns of each CEMC were summed again with appropriate weights proportional to the distance of a column from the beam axis to form a signal that was proportional to the sum of the transverse momenta of photons hitting the CEMC. Two of these signals, the high p_T-trigger signals, were formed independently for each CEMC. If at least one of these two signals exceeded some given threshold, the event was recorded. Thus, the high p_T-trigger signal allowed a selection of the p_T for each event and suppressed recording of lower-p_T events. The highest p_T-trigger threshold used was slightly greater than 2 GeV/c.

Some events in the CEMC contained overlapping electromagnetic showers from the two photons in π^0 decay. The energies and positions of the photons were determined using a special reconstruction program, which included an experimentally measured electromagnetic shower shape. The shower shape was presented as a two-dimensional table of energy deposition from an electromagnetic shower as a function of the x and y positions relative to the center of the lead-glass counter. This table was defined by averaging the energy fluctuations of 2×10^5 positron events at spatial locations measured by a proportional wire chamber in front of the CEMC. The special reconstruction algorithm for the separation of overlapping showers was developed to decrease drastically the computer processing time compared to standard minimization procedures.

Overlapping showers were separated using the following method. A region of 3×3 lead-glass counters was defined, where up to 98% of the energy for a single electromagnetic shower was deposited, which was well described by the average shower shape from the shower-shape table. Three values were defined that described the shower: the energy, from the zero moment of the energy distribution, and the X and Y coordinates, from the center of gravity or first moments of the distribution. If the energy shower was not well described by the average shower shape, it was considered to be produced by two overlapping showers. In this case, five values were defined for each shower. In addition to the three described for a single shower, the widths in the X and Y directions or second moments were calculated from the energy distribution. These five measured values remained fixed while an iteration procedure was used to determine the values of the energies and pairs of coordinates for the two over-

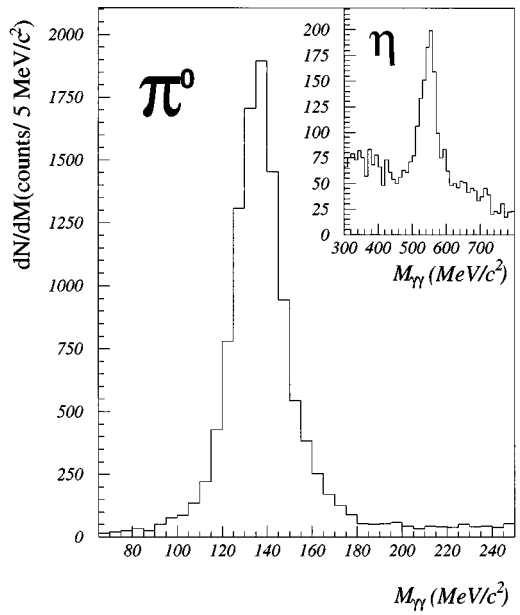

FIG. 2. The two-photon invariant-mass distributions for π^0 and η production by protons for the p_T region from 2.5 to 2.7 GeV/c.

lapping photon showers (six parameters). One of these six unknown values did not have any constraints, and it was the energy of one of the photons. It was an arbitrary choice. Once that was fixed, the other five variables were defined using the five measured moments. A parameter ρ, a type of χ^2, was defined to compare the iterative values with the shower shape table, and was minimized in the iteration procedure. This procedure then produced the energies and coordinates for the two overlapping photons. Further details of the π^0 reconstruction program are given in Ref. [14].

The following criteria were used to select π^0 candidates from all combinations of photon pairs: (1) The showers must be contained within a distance of at least one counter width away from the edge so that energy did not leak out of the calorimeter; (2) the asymmetry in the energies for the two photon showers, $A_E=|E_1-E_2|/(E_1+E_2)$, was less than 0.8 to reduce the combinatorial background; (3) the two-photon invariant mass was selected between 110 and 155 MeV/c^2 for $p_T<2.4$ GeV/c, and between 110 and 170 MeV/c^2 for $p_T>2.4$ GeV/c to account for the change in the width of the mass distribution; and (4) $-0.15\leqslant x_F\leqslant +0.15$.

A total of 2×10^7 events was recorded with incident protons and a total of 2×10^6 events with incident antiprotons. The analysis identified about $10^6\pi^0$ events satisfying the above criteria that were produced by protons tagged as positively or negatively polarized. An approximately equal number of π^0 events was produced by protons tagged with average polarization of zero. A total of $1.7\times10^5\pi^0$ events produced by polarized antiprotons was identified by the analysis. The measurement of the asymmetry of π^0 production associated with charged particles was made during the last 20% of the entire data-taking period.

Mass distributions constructed from pairs of photons are shown in Fig. 2. For each p_T bin mass distribution, the π^0 signal was described by a Gaussian curve and extracted from the combinatorial background, due mostly to pairs of uncorrelated photons, described by a third-order polynomial. A cut according to the value of ρ that compared the shower shape measured in a given event with an average electromagnetic shower shape suppressed hadron-induced showers by approximately a factor of 10. A background of about 7% was measured at low p_T and increased to about 26% at the highest p_T values measured in the experiment.

The mass resolution was found to be 21 MeV/c^2 (FWHM) at $p_T\approx1.5$ GeV/c, and contained contributions from the lead-glass spatial resolution of ±1.5 mm, the energy resolution of $\Delta(E)/E=0.03+0.25/\sqrt{E}$ (FWHM), and the target length. The mass resolution deteriorated with increasing p_T, for example, becoming 33 MeV/c^2 (FWHM) at $p_T\approx3.5$ GeV/c, due to an increase in the number of events that had shower overlap. Identical mass distributions were found for both CEMC1 and CEMC2, indicating that the absolute calibration and energy resolutions were the same in both detectors.

III. INVARIANT CROSS SECTIONS

In this section, the results from the measurements of the inclusive π^0 production cross sections averaged over the range $-0.15<x_F<+0.15$ are presented. The invariant cross section $Ed^3\sigma/dp^3$ was determined as

$$E\frac{d^3\sigma}{dp^3}=\frac{E}{2\pi p^z_{\max}p_T}\left[\frac{N^H_{\pi^0}}{N^H_{\rm tot}}-\frac{N^E_{\pi^0}}{N^E_{\rm tot}}\right]\frac{1}{\varepsilon_{\rm geom}}\frac{1}{\varepsilon_{\rm rec}}\times k_{\rm back}\frac{1}{\Delta p_T}\frac{1}{\Delta x_F}\frac{A}{N_A\rho l}, \tag{3}$$

where E is the energy of the π^0 in the c.m. system; $p^z_{\max}$ is the maximum π^0 c.m. longitudinal momentum of the $pp(\overline{pp})$ interaction ($p^z_{\max}\approx\sqrt{s}/2$, where s is the c.m. squared energy); p_T is the π^0 transverse momentum; $N^H_{\pi^0}$ and $N^E_{\pi^0}$ are the numbers of π^0's that survived the selection criteria described in the previous section for the hydrogen and empty targets, respectively; $N^H_{\rm tot}$ and $N^E_{\rm tot}$ are the numbers of beam particles for the hydrogen and the empty targets, respectively; $\varepsilon_{\rm geom}$ is the geometrical acceptance for π^0; $\varepsilon_{\rm rec}$ is the efficiency of the π^0 reconstruction algorithm; $k_{\rm back}$ is the ratio of ''pure'' π^0's to the total number of two photon pairs within the mass interval; Δp_T and Δx_F are the bins for the transverse momentum and the Feynman x_F variable, respectively; and $N_A\rho l/A$ is the number of hydrogen nuclei per cm^2 in the target. The p_T bin width was $\Delta p_T=0.2$ GeV/c and the x_F bin width was $\Delta x_F=0.3$. The number of hydrogen nuclei in the target was 4.23×10^{24} nuclei/cm^2.

The acceptance and the π^0 reconstruction efficiency were calculated using a Monte Carlo simulation program. This program generated π^0's with appropriate x_F and p_T distributions and then simulated the pattern of energy deposited in the detector using the shower profiles obtained from the positron beam calibration. The Monte Carlo–generated events were analyzed with the same shower reconstruction program as that used for actual events.

The ratio of the quantity $N^E_{\pi^0}/N^E_{\rm tot}$ to $N^H_{\pi^0}/N^H_{\rm tot}$, the normalized number of empty target to hydrogen target π^0 events, was 10% and did not depend on p_T in the region of

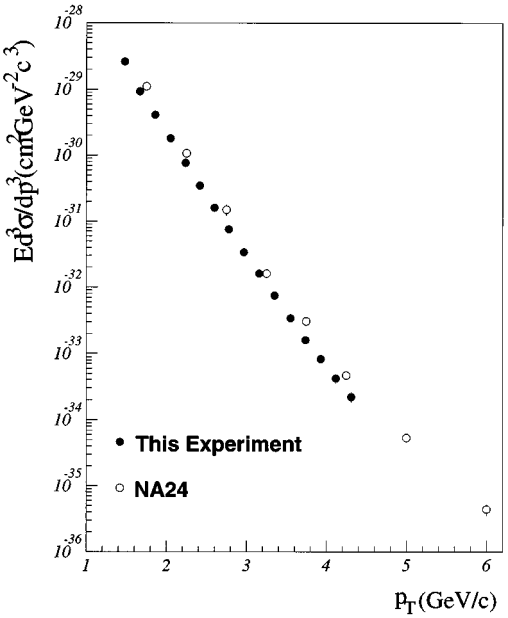

FIG. 3. The invariant cross sections for the reaction $p+p\rightarrow\pi^0+X$ at 200 GeV/c at $x_F=0$ (solid circles), and at 300 GeV/c at $x_F=0$ (open circles) from Ref. [18].

interest. The geometrical acceptance $\varepsilon_{\rm geom}$ increased from 8% at $p_T\approx1.5$ GeV/c to 26% at $p_T\approx4.5$ GeV/c for both calorimeters. The reconstruction efficiency $\varepsilon_{\rm rec}$, including the energy asymmetry cut $A_E=0.8$, changed slowly from 72% at $p_T\approx1.5$ GeV/c, to 66% at $p_T\approx3.5$ GeV/c, and then to 56% at $p_T\approx4.5$ GeV/c because the distance between two photons from π^0's decreased when p_T increased. The $k_{\rm back}$ ratio changed from 93% at $p_T\approx1.5$ GeV/c to 74% at $p_T\approx4.5$ GeV/c. This means that when p_T increased, the combinatorial background decreased slower than the π^0 production rate. The cross sections were multiplied by a factor of 1.07, which takes into account the proton beam absorption in a 1-m-long hydrogen target, and by another factor of 1.012, which takes into account the branching ratio of π^0 decay into two photons (98.8%).

The invariant unpolarized cross sections for inclusive π^0 production in pp interactions are shown in Fig. 3, where the errors shown are statistical only, and the results for both pp and $\overline{pp}$ interactions are presented in Table I. Uncertainties in the number of events from the hydrogen target dominated the statistical errors on the cross section. A statistical error of the background subtraction was also included, but was small. Systematic uncertainties in the geometrical acceptance, reconstruction efficiency, trigger efficiency, and the dummy target event count subtraction contributed to the point-to-point systematic errors of the cross sections. These errors were significantly higher (one order of magnitude) than the statistical ones at low p_T (see Table I) and then became comparable at higher p_T. An additional overall systematic uncertainty, associated with the beam and target, was estimated to be $\pm15\%$, and a p_T-scale uncertainty was estimated to be $\pm3\%$.

No significant differences were observed in a comparison of the π^0 production in pp and $\overline{pp}$ interactions. This agreement of pp and $\overline{pp}$ is consistent with the results obtained at $\sqrt{s}=24.3$ GeV/c [15]. The ratios of the spin-averaged invariant cross sections for π^0 production in pp and $\overline{pp}$ interactions were measured previously [16] with the same electromagnetic calorimeter but in a different kinematic region. These ratios were close to 1 when $x_F\rightarrow0$ and $1.4<p_T<2.0$ GeV/c, which is consistent with the current results.

The results from the current experiment on the invariant cross sections for the reaction $p+p\rightarrow\pi^0+X$ are in qualita-

TABLE I. Invariant cross sections $Ed^3\sigma/dp^3$ (in cm^2 GeV$^{-2}/c^3$) for inclusive π^0 production averaged over the x_F range from -0.15 to 0.15, with statistical and systematic errors given, respectively. There are additional systematic uncertainties of $\pm3\%$ in the p_T scale and $\pm15\%$ in the normalization. When calculating the ratio R of the two invariant cross sections, both statistical and systematic errors were taken into account.

p_T (GeV/c)	$p+p\rightarrow\pi^0+X$	$\overline{p}+p\rightarrow\pi^0+X$	$R_{\pi^0}(\overline{pp}/pp)$
1.48	$(3.12\pm0.008\pm0.36)\times10^{-29}$	$(2.88\pm0.02\pm0.24)\times10^{-29}$	0.92 ± 0.13
1.67	$(1.10\pm0.003\pm0.12)\times10^{-29}$	$(1.19\pm0.01\pm0.12)\times10^{-29}$	1.08 ± 0.16
1.86	$(4.89\pm0.014\pm0.35)\times10^{-30}$	$(5.72\pm0.08\pm0.47)\times10^{-30}$	1.17 ± 0.13
2.05	$(2.15\pm0.007\pm0.12)\times10^{-30}$	$(2.52\pm0.05\pm0.24)\times10^{-30}$	1.17 ± 0.13
2.24	$(9.37\pm0.04\pm0.73)\times10^{-31}$	$(1.11\pm0.03\ \pm0.09)\times10^{-30}$	1.18 ± 0.13
2.42	$(4.16\pm0.02\pm0.35)\times10^{-31}$	$(5.34\pm0.20\ \pm0.35)\times10^{-31}$	1.28 ± 0.14
2.60	$(1.90\pm0.015\pm0.12)\times10^{-31}$	$(2.51\ \pm0.14\ \pm0.12)\times10^{-31}$	1.32 ± 0.13
2.78	$(8.92\pm0.10\pm0.59)\times10^{-32}$	$(1.17\ \pm0.10\ \pm0.12)\times10^{-31}$	1.31 ± 0.16
2.97	$(4.02\pm0.06\pm0.23)\times10^{-32}$	$(3.90\ \pm0.47\ \pm0.23)\times10^{-32}$	0.97 ± 0.14
3.16	$(1.89\pm0.04\pm0.12)\times10^{-32}$	$(2.12\ \pm0.35\ \pm0.12)\times10^{-32}$	1.12 ± 0.21
3.35	$(8.85\pm0.27\pm0.59)\times10^{-33}$	$(8.38\ \pm2.36\ \pm0.59)\times10^{-33}$	0.95 ± 0.28
3.55	$(4.04\ \pm0.18\ \pm0.35)\times10^{-33}$		
3.74	$(1.90\ \pm0.12\ \pm0.12)\times10^{-33}$		
3.93	$(9.86\ \pm0.88\ \pm1.08)\times10^{-34}$		
4.12	$(4.96\ \pm0.49\ \pm0.59)\times10^{-34}$		
4.31	$(2.62\ \pm0.36\ \pm0.36)\times10^{-34}$		

TABLE II. Combination of CEMC, beam, and snake states corresponding to the normalized sums n^+ and n^-.

CEMC	Part of the beam	Snake status, corresponding to	
		n^+	n^-
1	Right	1	2
1	Left	2	1
2	Right	2	1
2	Left	1	2

tive agreement with the results of other experiments [17–19]. For comparison with our data in Fig. 3 the invariant cross section data from the NA24 experiment at CERN [18] are also shown. The NA24 data cover a greater p_T range, up to 6 GeV/c, and from that a clear change in the experimental slope from 4 to about 3 $(\mathrm{GeV}/c)^{-1}$ near $p_T=3.6$ GeV/c can be observed. The proton data from the current experiment also indicate this behavior. Fitting the cross section values by a single exponential curve e^{-bp_T} over the range $1.4<p_T<4.4$ GeV/c, the slope parameter b is (4.19 ± 0.08) $(\mathrm{GeV}/c)^{-1}$ with $\chi^2=2.14$ per degree of freedom. If two separate exponential curves are fit to the data, then $b=(4.3\pm0.1)$ $(\mathrm{GeV}/c)^{-1}$ in the region $1.4<p_T<3.6$ GeV/c, and (3.5 ± 1.2) $(\mathrm{GeV}/c)^{-1}$ for $3.6<p_T<4.4$ GeV/c, with $\chi^2=0.85$ per degree of freedom for both parts of the p_T region. Both statistical and systematic errors added in quadrature were taken into account.

IV. SINGLE-SPIN ASYMMETRIES

The left-right asymmetry $A_N(p_T)$ for a given CEMC is given by the expression

$$\frac{[n^+(p_T,\varphi)-n^-(p_T,\varphi)]}{[n^+(p_T,\varphi)+n^-(p_T,\varphi)]}=A_N(p_T)P_{\mathrm{beam}}\cos\varphi, \qquad (4)$$

where n^+ and n^- are the events with polarization and snake spin rotation states such that the final beam spin direction is aligned vertically up or down, respectively. The $n^+(n^-)$ values are normalized to the flux of particles passing through the target. The beam polarization P_{beam} was about 0.46.

A six-dimensional vector was accumulated for each event to determine the single transverse spin asymmetries. This matrix contained the transverse momentum p_T; the Feynman variable x_F; the azimuthal angle φ; the snake state, which describes the rotation of the spin; the CEMC that triggered the event; and the polarization state. Values were assigned within this matrix according to a given snake state, polarization state, and the triggered CEMC.

Four sets of asymmetries were calculated with four independent combinations of calorimeter and beam polarization, namely, CEMC1, CEMC2, and the positive and negative polarization parts of the beam. For each of these four methods, two snake states were used to calculate n^+ and n^- in Eq. (4), and presented in Table II. The final results were obtained by taking a weighted average of the four asymmetries with their errors. All four asymmetries are in good agreement with each other, within the statistical errors. Single-spin asymmetries

TABLE III. Asymmetries (1) in the pure inclusive reaction $p\uparrow+p\to\pi^0+X$ and (2) in the semi-inclusive reaction $p\uparrow+p\to\pi^0+X$ when at least one associated charged particle is produced at $(180\pm30)°$ relative to the π^0. The details of an estimate of statistical and systematic errors are in the text.

p_T (GeV/c)	(1) A_N (%)	(2) A_N (%)
1.09	$-0.8\pm0.4\pm0.4$	$-1.7\pm1.6\pm1.4$
1.29	$-0.7\pm0.5\pm0.4$	$-0.3\pm1.6\pm1.4$
1.48	$0.7\pm0.5\pm0.5$	$2.1\pm1.5\pm1.3$
1.67	$1.0\pm0.6\pm0.5$	$0.8\pm1.5\pm1.3$
1.86	$0.1\pm0.6\pm0.5$	$-1.2\pm1.6\pm1.4$
2.05	$-1.0\pm0.7\pm0.6$	$-2.0\pm1.7\pm1.5$
2.24	$0.6\pm0.9\pm0.8$	$-0.5\pm2.1\pm1.9$
2.42	$1.6\pm1.2\pm1.1$	$2.4\pm2.8\pm2.4$
2.60	$1.0\pm1.7\pm1.5$	$-2.9\pm3.8\pm3.3$
2.82	$-3.8\pm2.1\pm1.9$	$-9.8\pm4.7\pm4.2$
3.07	$3.2\pm4.1\pm3.6$	$4.5\pm9.2\pm8.2$
3.26	$-4.2\pm5.8\pm5.0$	$-16\pm13\pm11$
3.49	$1.1\pm7.2\pm6.3$	$-1\pm15\pm13$
3.78	$-6\pm12\pm10$	
4.12	$4\pm14\pm13$	

of inclusive π^0 production in pp interactions near 90°c.m. are presented in Table III and Fig. 4. Those asymmetries produced in $\overline{pp}$ interactions are given in Table IV and Fig. 5.

An updated analysis of the data was perfomed that (1) reconstructed the vertex for a fraction of the events, (2) recalibrated the energy scale of the CEMC using the π^0 and η^0 masses, (3) corrected the beam polarization decoding, which previously influenced the selection of good events and

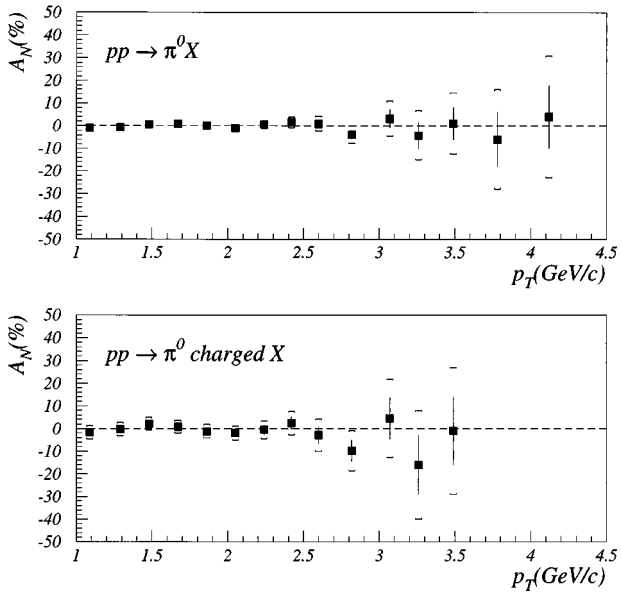

FIG. 4. The asymmetry parameter A_N as a function of p_T at $x_F=0$ (a) for the inclusive reaction $p\uparrow+p\to\pi^0+X$ and (b) for the same reaction, but when at least one charged particle is also detected at an azimuthal angle within $(180\pm30)°$ relative to the π^0.

TABLE IV. Asymmetries (1) in the pure inclusive reaction $p\,\overline{\uparrow}+p\rightarrow\pi^0+X$ and (2) in the semi-inclusive reaction $p\,\overline{\uparrow}+p\rightarrow\pi^0+X$ when at least one associated charged particle is detected at (180 ± 30)° relative to the π^0. The details of an estimate of statistical and systematic errors are in the text.

p_T (GeV/c)	(1) A_N (%)	(2) A_N (%)
1.09	$1.2\pm1.5\pm1.4$	$4.0\pm2.4\pm2.2$
1.29	$0.9\pm1.6\pm1.4$	$2.9\pm2.4\pm2.2$
1.48	$-2.6\pm1.8\pm1.6$	$-3.1\pm2.8\pm2.5$
1.67	$2.0\pm2.2\pm2.0$	$-4.7\pm3.6\pm3.3$
1.86	$-5.9\pm3.0\pm2.7$	$-3.1\pm5.0\pm4.5$
2.05	$2.2\pm4.2\pm3.8$	$12\pm7\pm6$
2.24	$-7.9\pm6.3\pm5.5$	$2\pm9\pm8$
2.42	$2.6\pm8.2\pm7.4$	$-2\pm14\pm13$
2.60	$8\pm12\pm11$	$2\pm18\pm16$
2.78	$-50\pm17\pm15$	$-50\pm28\pm25$
3.10	$-33\pm19\pm17$	$-1\pm33\pm29$

reduced the overall final sample by 30%, and (4) removed a cut on A_N for the zero-polarization part of the beam, which restored the 30% of the data, but then used these results to estimate systematic errors. In the $1<p_T<3$ GeV/c region, the current results agree well with those given previously [10], and are consistent with a zero value of the asymmetry. The statistics are large in this region, and the difference in the amount of data analyzed did not significantly influence the asymmetry values. However, in the $3<p_T<4.6$ GeV/c region, where the number of events is much smaller and the earlier asymmetry values deviated from zero by 2–3 standard deviations, all the analysis improvements mentioned above have changed the asymmetry values to zero within the errors. Over the whole p_T region, the previous asymmetry [10] was consistent with zero with a χ^2 of 3.0 per degree of freedom, and for the final asymmetry it has become 1.5.

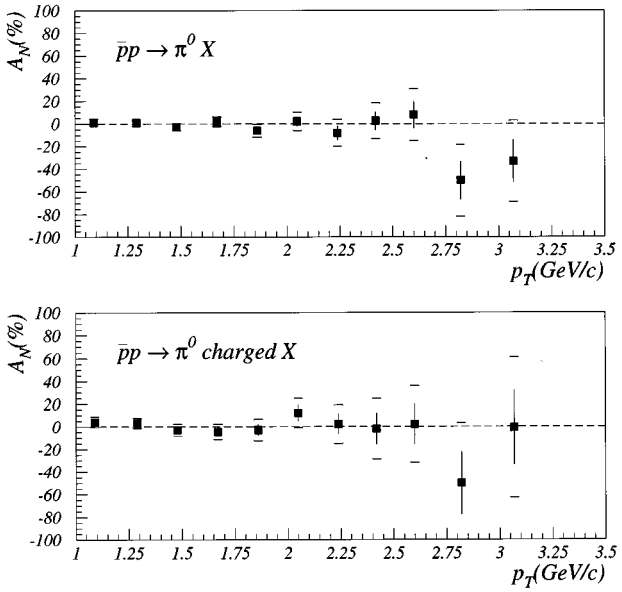

FIG. 5. The asymmetry parameter A_N as a function of p_T at $x_F=0$ (a) for the inclusive reaction $\overline{p\uparrow}+p\rightarrow\pi^0+X$ and (b) for the same reaction, but when at least one charged particle is also detected at an azimuthal angle (180 ± 30)° relative to the π^0.

In the previous analysis [10], there was an error in the polarization decoding as noted above. For the ''positive'' polarization part of the beam (+0.35 to +0.65), the decoding was performed correctly. For the ''negative'' polarization part of the beam, polarization values between −0.15 and −0.45 were used instead of −0.35 to −0.65, and for ''zero'' polarization, −0.45 to −0.65 and −0.15 to +0.35 were used instead of −0.35 to +0.35. In addition, about 30% of the runs were excluded based on a criterion that the zero-polarization data (''false asymmetry'') for all p_T bins in the run should differ from zero by less than about three standard deviations. In the revised analysis a different philosophy was adopted and such a criterion was not used. Instead, the ''false asymmetry'' results were used to estimate the systematic error for each p_T bin as described below. The ''false asymmetries'' were also generally smaller after the correction of the polarization decoding and the other two improvements to the analysis. None of the improvements or changes was found to be predominantly responsible for the difference between [10] and the present results for the values of A_N for the five p_T bins above 3 GeV/c.

The single transverse spin asymmetry could be sufficiently determined by only one CEMC, one of the two polarized portions of the beam, and the polarization reversal by the spin-rotation magnets. Two levels of redundancy were given by the parts of the beam polarized with opposite values and the left-right symmetry in the detector. Consistency among the four methods to calculate the asymmetry gave a check of the instrumental errors specific to each method. The statistical errors from the ''false'' asymmetries, calculated from the consistency checks, were used as an estimate of the systematic errors of the single-spin asymmetry for each point. The relative systematic error proportional to the A_N value was estimated to be 10% and was mainly due to the uncertainty in the beam polarization. No asymmetry was found using events with an average beam polarization of zero.

Semi-inclusive reactions with hard back-to-back production of two hadrons are interesting since they represent the underlying parton kinematics in a more transparent way. In addition to the inclusive reaction, $p\uparrow+p\rightarrow\pi^0+X$, the events were also selected that contained at least one charged particle having an azimuthal angle of $\varphi=(180\pm30)°$ relative to the produced π^0 direction. The single-spin asymmetries for inclusive π^0 production with an associated charged particle in pp interactions are given in Table III and Fig. 4. Those asymmetries produced in $\overline{pp}$ interactions are given in Table IV and Fig. 5.

Several tests were performed to check the quality of the data. One test investigated the possible appearance of bad events due to beam motion at the beginning of the spill. By eliminating the first 50 events of the spill, corresponding to removing 25% of all data events, asymmetries were again calculated. Removing these events did not significantly alter the asymmetry.

In the analysis, the pseudorapidity η was used instead of the Feynman variable x_F, and a $|\eta|<0.4$ region was integrated rather than a $|x_F|<0.15$ region. These differences did not affect the result.

V. DISCUSSION

The present results for the one-spin asymmetry $A_N(p_T)$ in π^0 production by polarized protons at 200 GeV/c can be compared to the previous measurements of $A_N(p_T)$ in inclusive pion production with initial energies from 13 to 40 GeV at $x_F=0$ and $p_T<3$ GeV/c, using transversely polarized proton beams or targets. The Brookhaven experiment [1] had studied π^+ production at 13.3 and 18.5 GeV. The CERN-PS [2] and Serpukhov [3] experiments had measured π^0 production by 24-GeV protons and 40-GeV negative pions, respectively. In all these experiments the asymmetries were small at low p_T and then rose to relatively large positive values. A positive sign of A_N corresponds to a larger production cross section to the beam left (beam right) when the beam (target) proton spin is aligned vertically upward. The similarity between π^+ and π^0 production asymmetries may be expected considering that both involve valence u-quark scattering. Observations [3,20] showed that at energies from 13.3 to 40 GeV, the rise of $A_N(p_T)$ to large positive values occurred at fixed values of the transverse scaling variable, $x_T=0.4$. This particular x_T value was interpreted [3] as a point x_T^0 where the relative phase of two helicity amplitudes goes to zero, and perhaps changes sign. This seems to be clearly supported by the experimental data in the beam momentum range from 13 to 40 GeV/c.

In some polarization measurements, a strong correlation has been observed [21–24] between a change of exponential slope in the cross section data and some change in the asymmetry. For example, previous measurements of the polarization parameter in an exclusive charge-exchange reaction, $\pi^- + p\uparrow \rightarrow \pi^0 + n$, or in the production of $\eta(550)$, $\omega(783)$, or $f(1270)$ mesons, exhibit this correlation. Since a break in the exponential slope of the differential production cross sections near $p_T=3.6$ GeV/c, initially observed by the NA24 group [18], is also suggested by the present measurements, the asymmetry $A_N(p_T)$ may show a change around this p_T value. Such a change in the asymmetry is not precluded by the large error bars in Table III. By extrapolating the x_T^0 scaling observed at low energies to 200 GeV/c, one would expect that the asymmetry should start to rise to positive values from zero somewhere near $p_T=4$ GeV/c.

The asymmetry is observed to be zero for single-spin inclusive π^0 production in pp interactions in the $1<p_T<3$ GeV/c region within a statistical accuracy up to 0.02. As mentioned previously, in perturbative QCD single-spin transverse asymmetries are expected to be practically zero. This expectation in the $1<p_T<3$ GeV/c region is confirmed by the data from this experiment, if perturbative QCD (PQCD) is applicable to these p_T values at 200 GeV. At larger p_T, the statistical errors grow from 0.05 at $p_T\approx 3.3$ GeV/c up to 0.15 at $p_T\approx 4.1$ GeV/c. After the more thorough data analysis, including the correction of the error in the polarization decoding, the present results are also consistent with zero. The new data supercede the preliminary measurements given in [10], where several points differed from zero by 2–3 standard deviations above $p_T=3$ GeV/c. More precise data are needed in the high-p_T region.

No significant difference in the asymmetry was observed when selected events were chosen with at least one additional charged particle, produced at $(180 \pm 30)^\circ$ relative to the π^0 direction. By investigating this reaction with the criteria chosen above, the fraction of hard parton-parton interactions could be enhanced. For this reaction, the asymmetry would not be as diluted by soft processes. The observed asymmetry was also consistent with zero.

The amount of data for studying $\overline{pp}$ interactions was an order of magnitude less than that for pp interactions. The asymmetry is equal to zero within the statistical accuracy for the $1<p_T<3$ GeV/c region.

The observations of a small or zero asymmetry at large p_T agree with the recent calculation of a twist-3 effect [9]. The higher-twist contribution to the single-spin effect in π^0 production at $x_F=0$ is not large. It also agrees with the model of an orbiting valence quark around a polarization axis that produces a zero asymmetry value at $x_F=0$, but a large asymmetry at large x_F values [25].

There is a QCD-based hard-scattering model [26] which can lead to single-spin asymmetries if one takes into account the transverse momenta of the constituents in a polarized proton . In contrast with PQCD, an asymmetry in this model does not depend on the small parameters like the quark mass and the strong coupling constant, but is proportional to the average value of the transverse momentum of the constituents. In the p_T region greater than 3 GeV/c our experimental data on asymmetry are qualitively consistent with the predictions of the model.

In the model for inclusive processes based on the U matrix, it is predicted that the single-spin asymmetry decreases while the energy increases [27]. The expected value of the asymmetry in this model is at the level of a few percent at 200 GeV, which does not contradict the current data results.

ACKNOWLEDGMENTS

We would like to acknowledge useful discussions of theoretical issues with colleagues at our respective institutions. We gratefully acknowledge the assistance of the staff of Fermilab and all the participating institutions. This work was performed at the Fermi National Accelerator Laboratory, which is operated by University Research Associates, Inc., under Contract No. DE-AC02-76CH03000 with the U.S. Department of Energy. This work was supported in part by the U.S. Department of Energy, Division of High Energy Physics, Contracts Nos. W-31-109-ENG-38, W-7405-ENG-36, and DE-AC02-76ER02289, DE-AS05-76ER05096. This research was also supported by the Ministry of Russian Federation on Atomic Energy, the Ministry of Education, Science and Culture in Japan, the Commissariat à l'Enérgie Atomique and the Institut de Physique Nucleaire et de Physique des Particules in France, and the Istituto di Fisica Nucleare in Italy.

[1] S. Saroff *et al.*, Phys. Rev. Lett. **64**, 995 (1990).
[2] J. Antille *et al.*, Phys. Lett. **94B**, 523 (1980).
[3] V. D. Apokin *et al.*, Phys. Lett. B **243**, 461 (1990).
[4] K. Heller, in *High Energy Spin Physics*, Proceedings of the VII International Symposium Protvino, Russia, 1986, edited by A. A. Antipova (Institute of High Energy Physics, Serpukhov, Russia, 1987), Vol. 1, p. 81.
[5] G. Kane, J. Pumpkin, and W. Repko, Phys. Rev. Lett. **41**, 1698 (1978).
[6] A. V. Efremov and O. V. Teryaev, Yad. Fiz. **36**, 242 (1982) [Sov. J. Nucl. Phys. **36**, 140 (1982)].
[7] M. G. Ryskin, Yad. Fiz. **48**, 1114 (1988) [Sov. J. Nucl. Phys. **48**, 708 (1988)].
[8] J. Qiu and G. Sterman, Phys. Rev. Lett. **67**, 2264 (1991).
[9] A. Schäfer, L. Mankiewicz, P. Gornicki, and S. Güllenstern, Phys. Rev. D **47**, R1 (1993).
[10] D. L. Adams *et al.*, Phys. Lett. B **276**, 531 (1992).
[11] D. P. Grosnick *et al.*, Nucl. Instrum. Methods Phys. Res. A **290**, 269 (1990).
[12] D. C. Carey *et al.*, Phys. Rev. Lett. **64**, 357 (1990).
[13] N. Akchurin *et al.*, Phys. Lett. B **229**, 299 (1989); N. Akchurin *et al.*, Phys. Rev. D **48**, 3026 (1993).
[14] D. L. Adams *et al.*, Report No. IHEP 91-99, 1991 (unpublished).
[15] J. Antille *et al.*, Phys. Lett. B **194**, 568 (1987).
[16] D. L. Adams *et al.*, Phys. Lett. B **261**, 201 (1991).
[17] G. Donaldson *et al.*, Phys. Lett. **73B**, 375 (1978).
[18] C. De Marzo *et al.*, Phys. Rev. D **36**, 16 (1987).
[19] F. W. Büsser *et al.*, Nucl. Phys. **B106**, 1 (1976).
[20] D. Sivers, Phys. Rev. D **43**, 261 (1991).
[21] V. D. Apokin *et al.*, Nucl. Phys. **B255**, 253 (1985).
[22] V. D. Apokin *et al.*, Z. Phys. C **35**, 173 (1987).
[23] I. A. Avvakumov *et al.*, Yad. Fiz. **42**, 1146 (1985) [Sov. J. Nucl. Phys. **42**, 725 (1985)].
[24] V. D. Apokin *et al.*, Yad. Fiz. **47**, 727 (1988) [Sov. J. Nucl. Phys. **47**, 465 (1988)].
[25] C. Boros, L. Zuo-tang, and M. Ta-chung, Phys. Rev. Lett. **70**, 1751 (1993).
[26] D. Sivers, Phys. Rev. D **41**, 83 (1990).
[27] S. M. Troshin and N. E. Tyurin, Phys. Rev. D **52**, 3862 (1995).